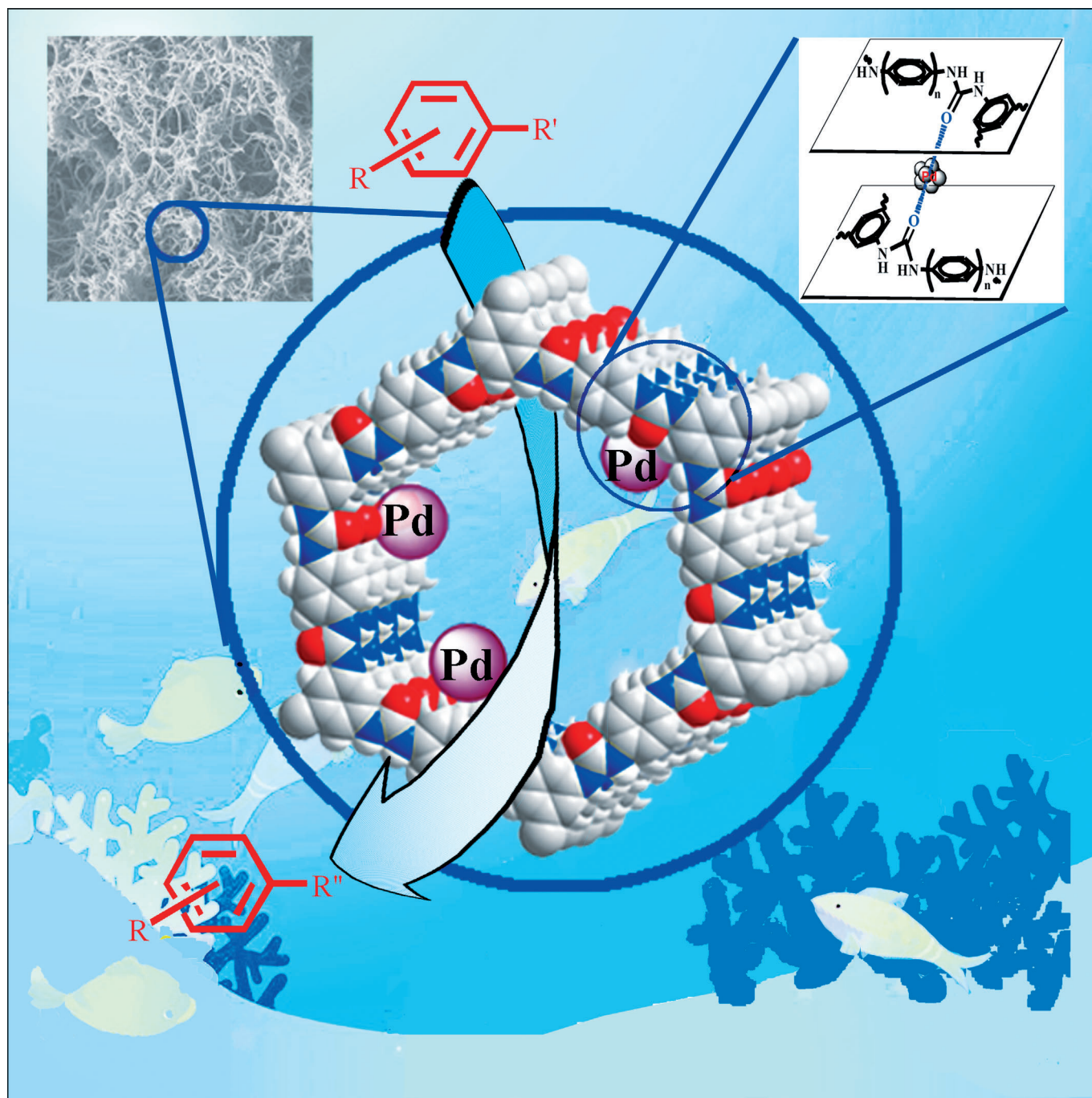


Sustainable Catalysis

Urea-Based Porous Organic Frameworks: Effective Supports for Catalysis in Neat Water

Liuyi Li, Zhilin Chen, Hong Zhong, and Ruihu Wang*^[a]



Abstract: Two urea-based porous organic frameworks, UOF-1 and UOF-2, were synthesized through a urea-forming condensation of 1,3,5-benzenetriisocyanate with 1,4-diaminobenzene and benzidine, respectively. UOF-1 and UOF-2 possess good hydrophilic properties and high scavenging ability for palladium. Their palladium polymers, Pd^{II}/UOF-1 and Pd^{II}/UOF-2, exhibit high catalytic activity and selectivity for Suzuki–Miyaura cross-coupling reactions and selective reduction of nitroarenes in water. The catalytic reactions can be

efficiently performed at room temperature. Palladium nanoparticles with narrow size distribution were formed after the catalytic reaction and were well dispersed in UOF-1 and UOF-2. XPS analysis confirmed the coordination of the urea oxygen atom with palladium. SEM and TEM images showed that the original network morphology of UOF-1 and UOF-2 was maintained after palladium loading and catalytic reactions.

Introduction

Porous organic frameworks (POFs) have received great interest owing to their unique features, such as high chemical stability, a large surface area, permanent porosity, and a modular synthetic procedure.^[1] With a growing need in emerging applications,^[2] various POFs with tailored functionalities have been constructed by deliberately selecting building blocks with desirable functional groups.^[3] In this context, POFs containing metal-binding sites, such as bipyridine,^[4] triazine rings,^[5] metalloporphyrins,^[6] imines,^[7] and salen,^[8] have been widely used as catalytic supports in oxidation reactions, photocatalysis, CO₂ conversions, and Suzuki–Miyaura cross-coupling reactions.^[9] But these reactions are usually performed either in organic or mixed organic/aqueous solvents.^[10]

Water is a cheap, safe, and nontoxic reaction medium and has thus attracted considerable attention. Generally, the efficient implementation of heterogeneous catalysis in water requires good aqueous dispersion of catalytic supports. However, the majority of POFs mainly consist of hydrophobic aromatic frameworks, which prevents their effective dispersion in water and results in poor contact between the substrate and the active sites. A feasible solution for overcoming the limitations is to increase the affinity of POFs with water by introducing hydrophilic linkages into the hydrophobic frameworks.^[11] Although the use of hydrophobic POFs in storage and separation applications has been widely investigated,^[2h,12] studies of POFs that contain hydrophilic linkages and their applications in heterogeneous catalysis in water have rarely been explored.

The urea group is known for its affinity with water. A urea-forming condensation reaction can be readily performed under mild conditions without releasing byproduct molecules.^[13] The relatively low cost of the starting materials and avoidance of precious-metal-catalyzed coupling chemistry make the urea group an appealing linkage for the construction of POFs. Urea linkages can be used as binding sites for transition metals,^[14]

which is beneficial for the stabilization of metal ions and nanoparticles in POFs through coordination interactions with urea. In addition, the surrounding phenyl rings in urea-based POFs can provide hydrophobic channels and void spaces that allow organic species to efficiently penetrate and be absorbed into POFs,^[15] which results in a microenvironment with high concentration of organic substrates inside the frameworks. These unique properties are expected to induce a positive effect on organic transformations in water. However, applications of urea-based POFs in heterogeneous catalysis in water have not been reported to date.

In our recent studies, we prepared a series of water-soluble palladium complexes by the attachment of hydrophilic groups, such as carboxylic acid and ammonium, to hydrophobic ligands. These complexes have demonstrated good catalytic activities in Suzuki–Miyaura cross-coupling reactions in water, but the separation difficulty of palladium catalysts results in poor recyclability of the catalytic systems.^[16] As a continuous effort to develop highly efficient and recyclable catalytic protocols,^[17] herein we report two urea-based POFs (UOF-1 and UOF-2), which were prepared by a facile urea-forming condensation of 1,3,5-benzenetriisocyanate with 1,4-diaminobenzene and benzidine, respectively. They were used as effective supports in palladium-catalyzed Suzuki–Miyaura cross-coupling reactions and reduction of nitroarenes in water, and the reactions can even be efficiently performed at room temperature.

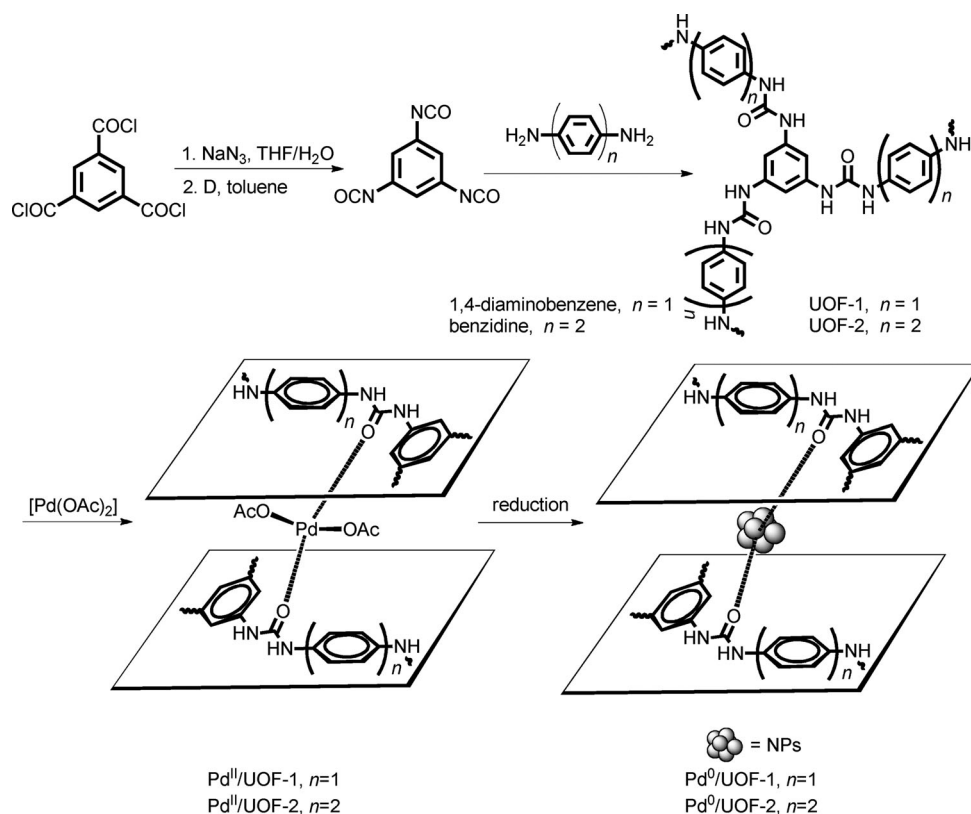
Results and Discussion

The synthetic route to UOF-1 and UOF-2 is shown in Scheme 1. Treatment of 1,3,5-benzenetricarbonyl trichloride with sodium azide followed by a Curtius rearrangement of thermolysis gave rise to 1,3,5-benzenetriisocyanate and a subsequent urea-forming condensation of 1,3,5-benzenetriisocyanate with 1,4-diaminobenzene and benzidine resulted in formation of UOF-1 and UOF-2, respectively. UOF-1 and UOF-2 are fluffy powders that are insoluble in water and common organic solvents.

UOF-1 and UOF-2 were characterized by using IR spectroscopy, solid-state ¹³C NMR spectroscopy, elemental analysis, thermogravimetric analysis (TGA), XRD, SEM, and TEM. In IR spectra of UOF-1 and UOF-2 (Figure S1 in the Supporting Information), disappearance of the stretching band of isocyanate at 2267 cm⁻¹ and concomitant emergence of the stretching band of C=O at 1665 cm⁻¹ indicated complete condensation be-

[a] Dr. L. Li, Dr. Z. Chen, Dr. H. Zhong, Prof. Dr. R. Wang
Key Laboratory of Coal to Ethylene Glycol and Its Related Technology
State Key Laboratory of Structural Chemistry
Fujian Institute of Research on the Structure of Matter
Chinese Academy of Sciences, Fuzhou, Fujian 350002 (China)
E-mail: ruihu@fjirsm.ac.cn

Supporting information for this article is available on the WWW under <http://dx.doi.org/10.1002/chem.201304046>.



Scheme 1. Synthesis of UOFs and the corresponding palladium polymers.

tween trisocyanate and the diamines. Solid-state ^{13}C NMR spectra further confirmed the presence of a carbonyl carbon atom of the urea moiety at $\delta = 155$ ppm, whereas other peaks at $\delta = 139$, 126, 118, and 105 ppm were assigned to carbon atoms of the aryl rings (Figure 1). The broad linewidths suggest that the carbon atoms have a heterogeneous surrounding. XRD further confirmed their amorphous structures (Figure S2 in the Supporting Information). Elemental analyses of UOF-1 and UOF-2 showed that the experimental values of C and N are slightly lower than the corresponding theoretical values; this deviation mainly resulted from the presence of trapped guest molecules, which is common in porous materials. The presence of guest molecules was further supported by TGA; initial weight losses of 4.6 and 3.1% up to 100 °C were observed for UOF-1 and UOF-2, respectively, and the frameworks of UOF-1 and UOF-2 were stable up to 221 and 238 °C, respectively (Figure S3 in the Supporting Information). Their morphology was examined by using SEM (Figure 2a, b and Figure S4a and b in the Supporting Information) and TEM (Figure 2c, d and Figure S5 in the Supporting Information). Interestingly, UOF-1 and UOF-2 exhibited 3D network morphology, which is much different from the granular morphology seen in most of the reported POFs.^[18]

The porous nature of UOF-1 and UOF-2 was studied by using N_2 adsorption measurements at 77 K. As shown in Figure S6a in the Supporting Information, the N_2 physisorption isotherms of UOF-1 and UOF-2 showed type IV isotherm patterns according to the IUPAC classification.^[19] A sharp rise at

high relative pressure in the N_2 adsorption isotherm showed the presence of large pores, which was ascribed to interparticle porosity. The appearance of hysteresis demonstrated deformation and swelling of the networks.^[20] The specific surface areas calculated from Brunauer–Emmett–Teller (BET) models of UOF-1 and UOF-2 were 113 and 91 $m^2 g^{-1}$, respectively. This unexpectedly low surface area probably results from framework interpenetration. The hydrogen bonds between urea–urea are probably responsible for interpenetration during the framework formation. The pore sizes of the two samples, calculated by appropriate fitting of density functional theory (DFT) model to the isotherm, were centered at 1.3 nm (Figure S6b in the Supporting Information).

Given that urea moieties may impart hydrophilic character to the polymers, the dispersion of polymers in H_2O and hexane was investigated to probe the hydrophilicity of the urea-containing polymers.^[11,21] As shown in Figure S7 in the Supporting Information, UOF-1 and UOF-2 were well distributed in water, and they were retained in the aqueous phase in a water/hexane biphasic system owing to the affinity of urea moieties to H_2O . The wettability was further investigated by examining the water contact angle (CA) measurements (Figure 3). The CA between water and UOF-1 is 60°. However, when a droplet of salad oil was placed on the surface of UOF-1, the oil was quickly adsorbed and the CA became almost 0°. The strong oleophilicity of the two polymers was ascribed to the presence of hydrophobic compositions of phenyl rings and the porous structure of UOF-1. These results demonstrated that UOF-1 and UOF-2 are good supports for catalysis in water because most substrates are hydrophobic in catalytic reactions.

UOF-1 was selected to test the scavenging ability for palladium. As shown in Figure S8 in the Supporting Information, when a suspension of UOF-1 was stirred in a solution of $[Pd(OAc)_2]$ in dichloromethane or in aqueous $PdCl_2$ with a palladium/urea molar ratio of 1:10, the yellowish supernatant became colorless, which suggests a good affinity of UOF-1 for palladium.

To investigate the coordination properties of palladium with urea units, $Pd^{II}/UOF-1$ and $Pd^{II}/UOF-2$ were prepared through a simple treatment of UOF-1 and UOF-2 with $[Pd(OAc)_2]$ in dichloromethane (Scheme 1). $Pd^{II}/UOF-1$ and $Pd^{II}/UOF-2$ are yellow powders. In their solid-state ^{13}C NMR spectra, the chemical shifts of the phenyl rings and urea units are almost identi-

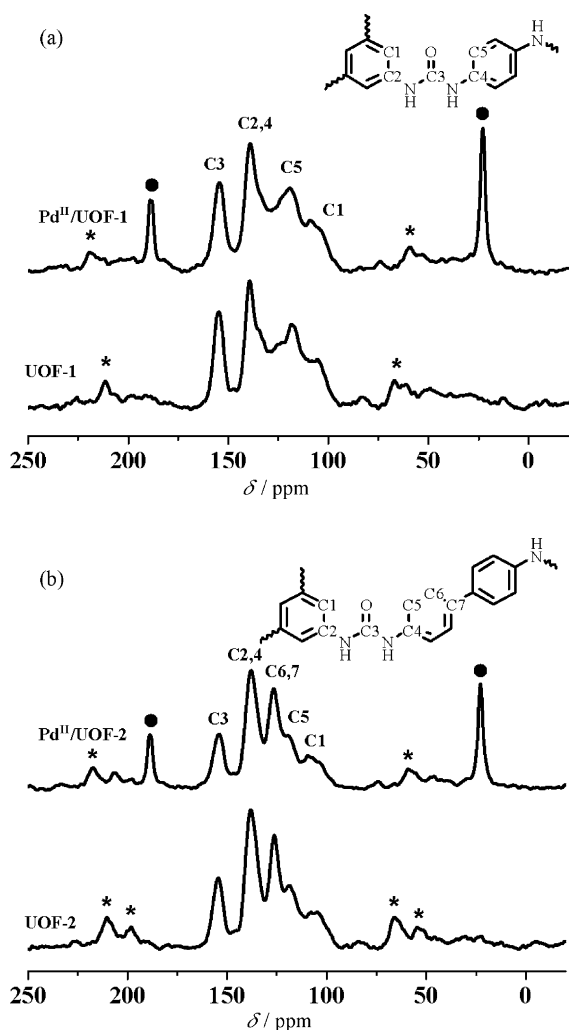


Figure 1. ^{13}C CP/MAS NMR spectra for: a) UOF-1 and Pd^{II} /UOF-1, and b) UOF-2 and Pd^{II} /UOF-2; * = spinning side bands.

cal to their respective precursors (Figure 1). Two new strong signals at $\delta = 188$ and 23 ppm are assigned to the characteristic peaks of carbonyl and methyl of the incorporated $[\text{Pd}(\text{OAc})_2]$, respectively. In comparison with the carbonyl peak of free $[\text{Pd}(\text{OAc})_2]$ at $\delta = 190$ ppm,^[7a] the chemical shift of the carbonyl group in the incorporated $[\text{Pd}(\text{OAc})_2]$ was shifted toward high field by $\delta = 2$ ppm, which suggests weak coordination of palladium with urea units. However, no characteristic bands for $[\text{Pd}(\text{OAc})_2]$ were observed at $1600\text{--}1650\text{ cm}^{-1}$ in the IR spectra of Pd^{II} /UOF-1 and Pd^{II} /UOF-2 owing to overlap of the $\text{C}=\text{O}$ stretching band of the urea moieties. Interestingly, SEM analyses showed that the incorporation of palladium have no obvious effect on their morphology (Figure 2e, f and Figure S4c and d in the Supporting Information), suggesting high physicochemical stability of Pd^{II} /UOF-1 and Pd^{II} /UOF-2.

To further investigate possible interactions between palladium and the urea units, XPS analyses were performed. As shown in Figure 4a and b, the binding energy of $\text{Pd}3\text{d}_{5/2}$ in Pd^{II} /UOF-1 and Pd^{II} /UOF-2 was 338.14 and 338.23 eV, respectively, which are assigned to the $+2$ oxidation state. In com-

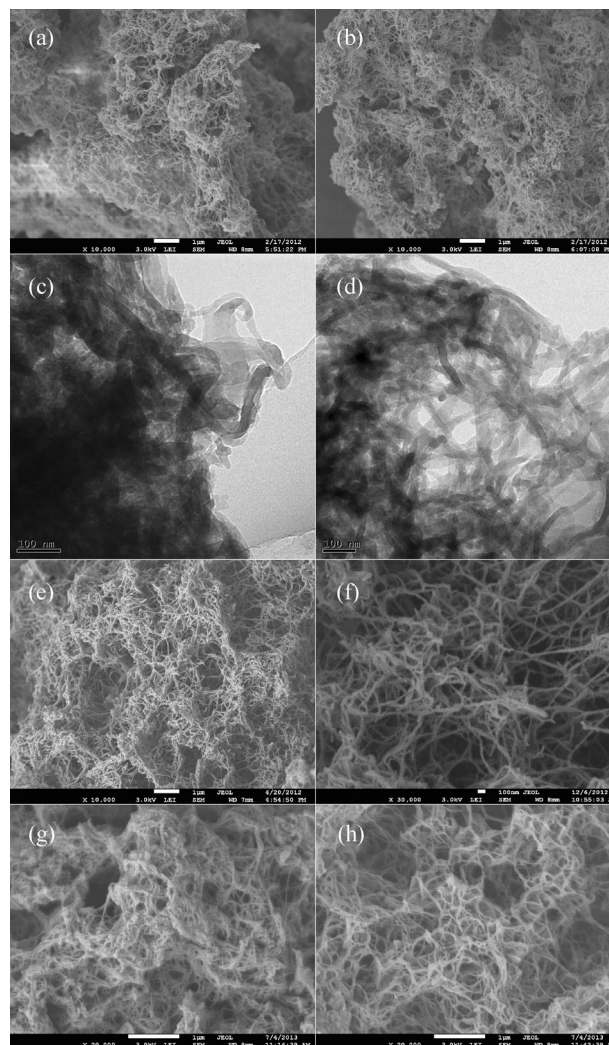


Figure 2. SEM images for: a) UOF-1 and b) UOF-2; TEM images for: c) UOF-1 and d) UOF-2; and SEM images for: e) Pd^{II} /UOF-1, f) Pd^{II} /UOF-2, g) Pd^0 /UOF-1, and h) Pd^0 -reduction. Scale bars: $1\ \mu\text{m}$ (a, b, e, g, h) and $100\ \text{nm}$ (c, d, f).

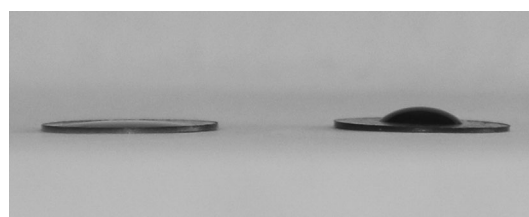


Figure 3. Images for contact angle measurement: Left: photograph of a salad oil droplet, and right: photograph of a water droplet on a sample of UOF-1.

parison with that of free $[\text{Pd}(\text{OAc})_2]$ (338.40 eV),^[7a] $\text{Pd}3\text{d}_{5/2}$ peaks in Pd^{II} /UOF-1 and Pd^{II} /UOF-2 were negatively shifted by about 0.26 and 0.17 eV, respectively, due to the interactions of $[\text{Pd}(\text{OAc})_2]$ with the frameworks. In comparison with UOF-1 and UOF-2, the binding energy of $\text{O}1\text{s}$ in Pd^{II} /UOF-1 and Pd^{II} /UOF-2 was shifted from 531.57 to 531.94 eV and from 531.99 to 532.98 eV, respectively, whereas the binding energy of $\text{N}1\text{s}$ re-

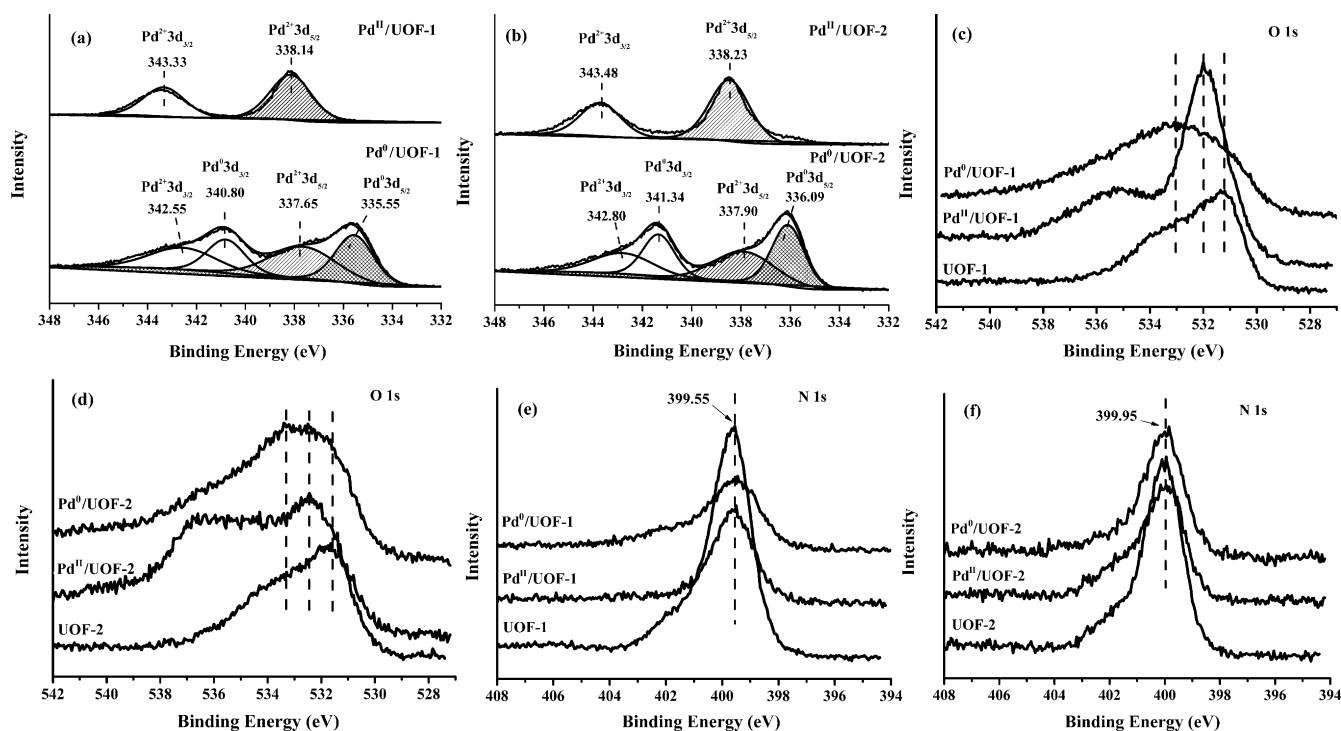


Figure 4. Pd 3d XPS spectra for a) Pd^{II}/UOF-1 and Pd⁰/UOF-1, b) Pd^{II}/UOF-2 and Pd⁰/UOF-2; O 1s spectra for c) UOF-1, Pd^{II}/UOF-1, and Pd⁰/UOF-1, d) UOF-2, Pd^{II}/UOF-2, and Pd⁰/UOF-2; N 1s spectra for e) UOF-1, Pd^{II}/UOF-1, and Pd⁰/UOF-1; f) UOF-2, Pd^{II}/UOF-2, and Pd⁰/UOF-2.

mained at 399.55 eV (Figure 4c–f). The above results showed that [Pd(OAc)₂] was successfully immobilized in the frameworks through the coordination interaction of palladium with oxygen atoms of the urea moieties. Pd contents were determined by using ICP analyses in Pd^{II}/UOF-1 and Pd^{II}/UOF-2 and found to be 16.87 and 16.83 wt%, which corresponds to 1.59 and 1.58 mmol g⁻¹, respectively.

Catalytic performances of Pd^{II}/UOF-1 and Pd^{II}/UOF-2 were initially evaluated in a Suzuki–Miyaura cross-coupling reaction in water. When the reaction of 4-bromoacetophenone with phenylboronic acid was performed with K₂CO₃ as a base in the presence of 0.5 mol% Pd^{II}/UOF-1, complete conversion of 4-bromoacetophenone was observed at 60 °C in 3 h (Table 1, entry 1). The use of NEt₃ and KOH as bases also gave rise to 4-acetyldiphenyl in almost quantitative GC yields (Table 1, entries 2 and 3), whereas KOAc was slightly less efficient in the cross-coupling reaction and gave the target product in 63% GC yield under the same conditions (Table 1, entry 4). When palladium loading was decreased to 0.05 mol%, 4-acetylbiphenyl was obtained in 76% GC yield (Table 1, entry 5). Interestingly, the catalytic system was also efficient at 25 °C; when the reaction of 4-bromoacetophenone with phenylboronic acid was performed at 25 °C for 24 h, 4-acetylbiphenyl was formed in a 98% isolated yield (Table 1, entry 6). This was challenging to achieve even for the homogeneous catalytic systems in water.^[16]

To explore scope and generality of the catalytic system in water, a series of aryl bromides and aryl boronic acids with different steric and electronic characters were tested. The effect of varying aryl bromides was firstly investigated by using phe-

Table 1. Suzuki–Miyaura cross-coupling reaction catalyzed by Pd^{II}/UOF-1 and Pd^{II}/UOF-2.^[a]

Entry	[Pd]	R ¹	R ²	Base	Yield [%] ^[b]
1	Pd ^{II} /UOF-1	4-COCH ₃	H	K ₂ CO ₃	100 (97)
2	Pd ^{II} /UOF-1	4-COCH ₃	H	NEt ₃	100 (96)
3	Pd ^{II} /UOF-1	4-COCH ₃	H	KOH	97
4	Pd ^{II} /UOF-1	4-COCH ₃	H	KOAc	63
5 ^[c]	Pd ^{II} /UOF-1	4-COCH ₃	H	K ₂ CO ₃	76
6 ^[d]	Pd ^{II} /UOF-1	4-COCH ₃	H	K ₂ CO ₃	98 (98)
7	Pd ^{II} /UOF-1	4-NO ₂	H	K ₂ CO ₃	95 (92)
8	Pd ^{II} /UOF-1	4-OH	H	K ₂ CO ₃	100 (98)
9	Pd ^{II} /UOF-1	4-CHO	H	K ₂ CO ₃	100 (99)
10	Pd ^{II} /UOF-1	4-CN	H	K ₂ CO ₃	99 (99)
11 ^[e]	Pd ^{II} /UOF-1	4-COOH	H	K ₂ CO ₃	– (100)
12	Pd ^{II} /UOF-1	4-OCH ₃	H	K ₂ CO ₃	65
13	Pd ^{II} /UOF-1	4-COCH ₃	4-F	K ₂ CO ₃	100 (99)
14	Pd ^{II} /UOF-1	4-COCH ₃	4-CH ₃ O	K ₂ CO ₃	98 (98)
15	Pd ^{II} /UOF-1	4-COCH ₃	4-CH ₃	K ₂ CO ₃	100 (99)
16	Pd ^{II} /UOF-1	4-COCH ₃	3-CH ₃	K ₂ CO ₃	99 (99)
17	Pd ^{II} /UOF-1	4-COCH ₃	2-CH ₃	K ₂ CO ₃	100 (98)
18	Pd ^{II} /UOF-1	2-CH ₃	4-COCH ₃	K ₂ CO ₃	22
19	Pd ^{II} /UOF-2	4-COCH ₃	H	K ₂ CO ₃	97 (95)
20	Pd ^{II} /UOF-2	4-OH	H	K ₂ CO ₃	100 (96)
21	Pd ^{II} /UOF-2	4-NO ₂	H	K ₂ CO ₃	95 (93)
22 ^[f]	Pd ^{II} /UOF-1	–	H	K ₂ CO ₃	– (96)
23 ^[f]	Pd ^{II} /UOF-1	–	4-CH ₃ O	K ₂ CO ₃	– (95)

[a] Unless otherwise stated, the reactions were carried out by using aryl bromide (0.5 mmol), arylboronic acid (0.75 mmol), K₂CO₃ (1.0 mmol), and [Pd] (0.5 mol%) in H₂O (2 mL) for 3 h. [b] GC yield, isolated yields are given in parenthesis. [c] [Pd] (0.05 mol%) was used. [d] T = 25 °C, t = 24 h. [e] K₂CO₃ (1.5 mmol) was used. [f] 5-Bromo-2-hydroxybenzoic acid was used as a substrate, with K₂CO₃ (2.0 mmol) was used.

nylboronic acid as a substrate (Table 1, entries 7–12). The aryl bromides containing electron-withdrawing groups, such as $-\text{NO}_2$, $-\text{OH}$, $-\text{CHO}$, $-\text{CN}$, and $-\text{COOH}$, gave rise to desirable products in excellent isolated yields (Table 1, entries 7–11), whereas the use of electron-rich 4-bromoanisole provided 4-methoxybiphenyl in 65% GC yield under the same conditions (Table 1, entry 12). The cross-coupling reactions of 4-bromoacetophenone with electron-deficient and electron-rich aryl boronic acids were also carried out, the corresponding biaryl products were obtained in excellent isolated yields (Table 1, entries 13–17). Note that the reactions of 4-bromoacetophenone with *ortho*-, *meta*-, and *para*-methyl-substituted phenylboronic acid produced the target products in quantitative yields (Table 1, entries 14–16), which suggests the electronic and steric nature of aryl boronic acids have no obvious effect on the cross-coupling reactions. It should be mentioned that a quantitative yield was achieved in the coupling reaction of 4-bromoacetophenone with 2-methylphenylboronic acid (Table 1, entry 17), whereas the reaction of 2-bromotoluene with 4-acetophenylboronic acid only provided the same product in 22% GC yield (Table 1, entry 18). It should be mentioned that the use of Pd^{II} /UOF also gave the target products in excellent isolated yields similar to those from Pd^{II} /UOF-1 (Table 1 entries 19–21).

It is known that palladium nanoparticles (NPs) are usually involved in palladium-catalyzed cross-coupling reactions.^[22] To discern the catalytic active species in Suzuki–Miyaura cross-coupling reactions, after the reaction between 4-bromoacetophenone and phenylboronic acid was conducted in the presence of Pd^{II} /UOF-1 and Pd^{II} /UOF-2 in water, the resultant mixture was extracted with diethyl ether and then centrifuged. The residues were successively washed with water and ethanol to afford gray powders, which were ultrasonically dispersed in anhydrous ethanol for TEM analysis. The palladium NPs were well dispersed in the frameworks of UOF-1 and UOF-2, they were denoted as Pd^0 /UOF-1 and Pd^0 /UOF-2, respectively (Figure 5). Their average sizes were (4.9 ± 0.94) and (4.8 ± 1.1) nm, respectively, which are comparable with those formed after the catalytic reaction.^[7a,23] SEM analyses of the 3D network morphology of UOF-1 and UOF-2 showed no obvious change after the Suzuki–Miyaura cross-coupling reaction (Figure 2g and Figure S4e in the Supporting Information).

To get an insight into palladium NPs in the urea-based frameworks, Pd^0 /UOF-1 and Pd^0 /UOF-2 were further investigated by using IR spectroscopy and XPS. The IR spectra showed that the main characteristic peaks of Pd^0 /UOF-1 and Pd^0 /UOF-2 were similar to those of UOF-1 and UOF-2 (Figure S1 in the Supporting Information). The XPS spectra indicated that the Pd3d region was divided into two spin-orbital pairs (Figure 4a), which indicated the presence of two types of surface-bound palladium species. For Pd^0 /UOF-1, the binding energy peaks at 335.55 ($\text{Pd}3d_{5/2}$) and 340.80 eV ($\text{Pd}3d_{3/2}$) were assigned to the Pd^0 species, whereas the peaks at 337.65 ($\text{Pd}3d_{5/2}$) and 342.55 eV ($\text{Pd}3d_{3/2}$) were attributed to the Pd^{II} species. The ratio of surface Pd^0 to Pd^{II} , as determined by ratio of their relative peak areas, was 0.82. In comparison with XPS spectra of UOF-1 and UOF-2, the binding energy peak of N1s in Pd^0 /UOF-1 and Pd^0 /UOF-2 was not shifted and remains at

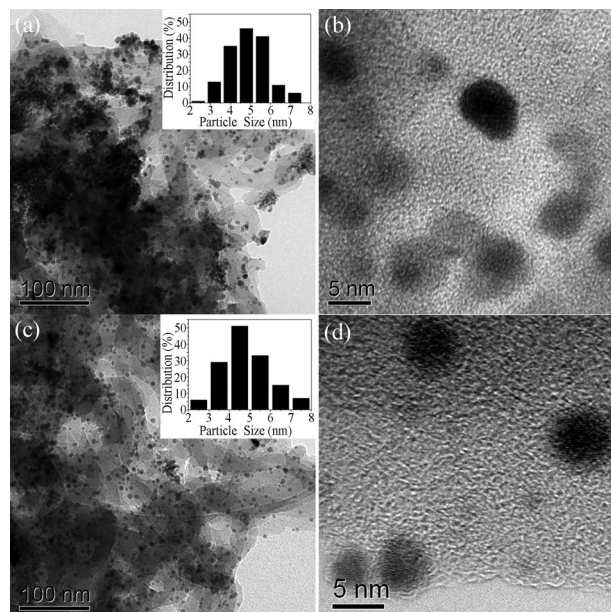
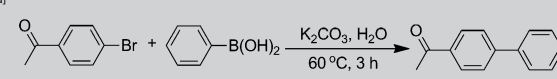


Figure 5. TEM images and palladium size distributions for: a, b) Pd^0 /UOF-1, and c, d) Pd^0 /UOF-2.

399.55 eV (Figure 4e), whereas the O1s peak in Pd^0 /UOF-1 and Pd^0 /UOF-2 was shifted from 531.57 to 532.99 eV and from 531.99 to 533.31 eV, respectively, due to coordination of the palladium NPs with oxygen atoms of the urea moieties. It should be mentioned that the O1s peak of the acetate group at 535.50 eV disappeared in Pd^0 /UOF-1 and Pd^0 /UOF-2, compared with that in Pd^{II} /UOF-1 and Pd^{II} /UOF-2.

To assess whether the catalytic system functions in a heterogeneous pathway, mercury drop test and poison experiments were carried out.^[24] When one drop of Hg^0 was added to the reaction mixture before the reaction of 4-bromoacetophenone and phenylboronic acid was performed, Pd^{II} /UOF-1 and Pd^{II} /UOF-2 provided 4-acetylbiphenyl in 83 and 70% GC yields, respectively (Table 2, entry 1), which was lower than that in the absence of mercury under the same conditions (Table 1, entries 1 and 19). The use of substoichiometric amount of CS_2 as a poisoning agent in catalysis has been reported to be strong evidence for the formation of NPs.^[25] No catalytic activity was detected when the reaction of 4-bromoacetophenone and phenylboronic acid was performed in the presence of 0.5 equivalent of CS_2 relative to palladium (Table 2, entry 2). Poly(vinylpyridine) (PVPy) has been shown to be an excellent scavenger for soluble palladium species due to its strong binding ability for palladium and insolubility in reaction media. However, nearly complete conversion of 4-bromoacetophenone was observed when 150 equivalent of PVPy was added to the catalytic system (Table 2, entry 3). The lack of effect of PVPy on the catalytic system was mainly ascribed to its inability to access active sites in pores of the frameworks. In contrast, the use of 150 equivalent of pyridine or PPh_3 as additives almost completely quenched the cross-coupling reaction (Table 2, entries 4 and 5). This is likely due to the fact that pyridine and PPh_3 , as small molecules, could enter freely into the

Table 2. Summary of poisoning experiments for Pd^{II}/UOF-1 and Pd^{II}/UOF-2.^[a]



Entry	Additive	Additive/Pd ratio	Conv. [%] ^[b]	Conv. [%] ^[c]
1	Hg	–	83	70
2	CS ₂	0.5	0	0
3	PVPy	150	99	99
4	pyridine	150	6	4
5	PPh ₃	150	5	0

[a] Reaction conditions: 4-bromoacetophenone (0.5 mmol), phenylboronic acid (0.75 mmol), K₂CO₃ (1.0 mmol), Pd^{II}/UOF-1 or Pd^{II}/UOF-2 (0.5 mol%) in H₂O (2.0 mL) at 60 °C for 3 h. [b] Pd^{II}/UOF-1. [c] Pd^{II}/UOF-2.

pores of the frameworks to poison the palladium active species. As a result, the catalytic system is heterogeneous. This argument was further confirmed by ICP analysis. After the reaction of 4-bromoacetophenone and phenylboronic acid was complete, ICP analyses showed that palladium leaching into the organic phase for Pd^{II}/UOF-1 and Pd^{II}/UOF-2 was 6.260 and 3.280 ppm, respectively, whereas palladium leaching to aqueous phase was 0.084 and 0.080 ppm, respectively. Owing to the negligible palladium leaching, the present catalytic system may be appropriate for synthesis of pharmaceutical precursors because the contamination of chemical intermediates by palladium residues is of great concern for development of large-scale syntheses, particularly in the pharmaceutical industry in which metal contaminants are strictly monitored.^[26] Biphenyl derivatives of salicylic acid are known pharmaceutical intermediates and possess high activity as tyrosinase inhibitors.^[27] To our delight, the catalytic system is also efficient for the synthesis of biphenyl derivatives of salicylic acid, and the reaction of 5-bromo-2-hydroxybenzoic acid with phenylboronic acid and 4-methoxyphenylboronic acid gave rise to the corresponding products in 96 and 95% isolated yields, respectively (Table 1, entries 22 and 23).

In addition to catalytic activity, recyclability is also crucial for an outstanding heterogeneous catalyst. The catalytic recyclability of Pd^{II}/UOF-1 and Pd^{II}/UOF-2 was evaluated by examining the reaction between 4-bromophenol and phenylboronic acid in the presence of 0.5 mol% palladium and K₂CO₃ at 60 °C for 3 h. After every cycle, the mixture was extracted with diethyl ether and the conversion of 4-bromophenol was determined by GC. The remaining water phase was centrifuged to afford a gray solid, which was further washed with ethanol and water and then employed in the next run with fresh substrates and base. Both Pd^{II}/UOF-1 and Pd^{II}/UOF-2 gave a complete conversion of 4-bromophenol in the first and second run (Figure 6). A slight loss in catalytic activity was observed in the fourth run for Pd^{II}/UOF-1, for which the target product was obtained in 90% GC yield, whereas the reactivity of Pd^{II}/UOF-2 began to decrease from the third run, so that 91 and 70% conversion of 4-bromophenol was obtained in the third and fourth runs, respectively.

Primary aromatic amines are widely used in the synthesis of natural products, pharmaceutical intermediates, polymers, and

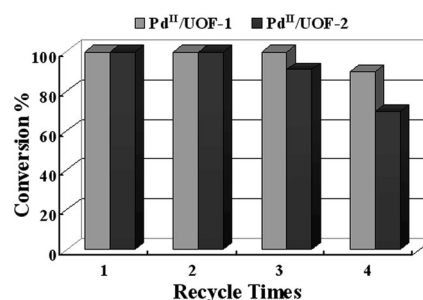


Figure 6. Recyclability of Pd^{II}/UOF-1 and Pd^{II}/UOF-2 in the Suzuki–Miyaura cross-coupling reaction. Reaction conditions: 4-bromophenol (0.5 mmol), phenylboronic acid (0.75 mmol), K₂CO₃ (1.5 mmol), and Pd^{II}/UOF-1 or Pd^{II}/UOF-2 (0.5 mol%) in H₂O (2.0 mL) at 60 °C for 3 h.

materials. Catalytic reduction of nitroarenes is one of the simple and efficient methods for the production of aromatic amines. The encouraging catalytic performances of Pd^{II}/UOF-1 and Pd^{II}/UOF-2 in Suzuki–Miyaura cross-coupling reaction prompted us to further explore their application in the selective reduction of nitroarenes. When the reduction reaction of nitrobenzene was performed with 0.5 mol% Pd^{II}/UOF-1 or Pd^{II}/UOF-2 as the catalytic precursor and three equivalent of NaBH₄ as a reductive reagent in water at room temperature, aniline was obtained in a full conversion in 1 h (Figure 7). After the reaction was complete, the resultant mixture was extracted with diethyl ether and the aqueous phase was centrifuged to afford a gray solid, which was further washed with ethanol and water and then used in the next run. Pd^{II}/UOF-1 maintained a catalytic activity of 100% in four consecutive runs, but the selectivity of aniline began to decrease from the third run; the selectivity of aniline in the third run and the fourth runs is 97 and 86%, re-

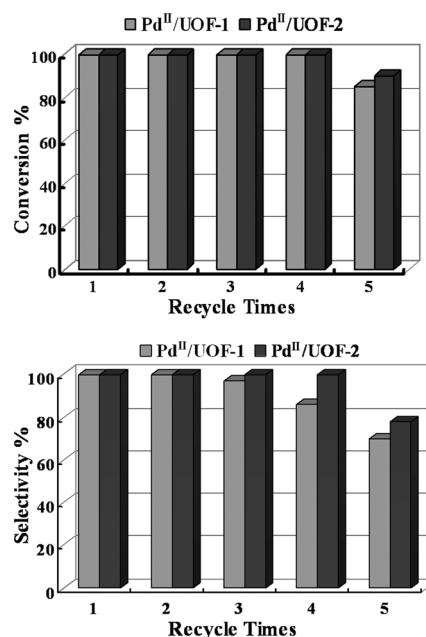


Figure 7. Reusability of Pd^{II}/UOF-1 and Pd^{II}/UOF-2 in catalytic reduction of nitrobenzene. Reaction conditions: nitrobenzene (1 mmol), Pd^{II}/UOF-1 or Pd^{II}/UOF-2 (0.5 mol%), H₂O (2.0 mL), and NaBH₄ (3 mmol) at 25 °C for 1 h.

spectively. The conversion of nitrobenzene and the selectivity of aniline in the fifth run were 80 and 70%, respectively. However, when Pd^{II}/UOF-2 was used four times, no obvious loss in catalytic activity and selectivity was observed, but the conversion of nitrobenzene and the selectivity of aniline in the fifth run were decreased to 90 and 78%, respectively.

Different nitro compounds were further used in the reduction of nitroarenes with Pd^{II}/UOF-2. When the reaction was performed in the presence of three equivalents of NaBH₄ in water at room temperature for 1 h, a variety of nitro compounds could be reduced to the corresponding amino compounds in high yield and selectivity (Table 3). Various functional groups, such as –OH, –NH₂, –OCH₃, –COOH, and –Cl, were well tolerated. Of these groups, electron-donating and -withdrawing groups have no obvious effect on the activity and selectivity of the reaction (Table 3, entries 1–7). In addition, *ortho*-, *meta*-, and *para*-methyl-substituted nitrobenzenes were selectively reduced into the corresponding products in quantitative yield (Table 3, entries 5–7), which suggests that electronic character and steric hindrance has no obvious effect on the catalytic system. Interestingly, the catalytic system is also effective for selective reduction of heterocyclic nitro compounds. If 4-nitroindole and 5-nitroindole were used as substrates, the corresponding products were obtained in 94 and 100% isolated yields, respectively (Table 3, entries 8 and 9). Notably, 1,3-dinitrobenzene can be completely reduced to 1,3-benzendiamine in quantitative isolated yield under the same conditions (Table 3, entry 10). Selective synthesis of 1,4-diaminobenzene

was also achieved in 96% isolated yield through reduction of 4-nitroaniline (Table 3, entry 11). It should be mentioned that reduction of 4-nitrobenzaldehyde gave rise to (4-aminophenyl)methanol in quantitative yield, in which CHO was concomitantly reduced, no side products of polyimine or polyamine were observed (Table 3, entry 12). Palladium catalysts are reported to possess a high tendency toward dehalogenation, so much effort was made to suppress side reactions through addition of inhibitors. However, the reduction of 4-nitrochlorobenzene and 2-nitrochlorobenzene gave rise to the corresponding products with 88 and 84% selectivity, respectively (Table 3, entries 13 and 14), in which the dechloro side-product aniline was obtained in 12 and 18% yield, respectively. As anticipated, when the reduction of nitrobenzene was performed in the absence of Pd^{II}/UOF-2 or with UOF-2 as a catalytic precursor, no aniline was detected under the same conditions (Table 3, entries 15 and 16), which suggests that the palladium catalytic species is necessary for the catalytic system.

After reduction of nitrobenzene in the presence of NaBH₄ and Pd^{II}/UOF-2 was complete, the resultant gray powder was denoted as Pd-reduction, and was analyzed by using SEM and TEM. SEM images showed that the morphology of Pd-reduction was identical to UOF-2 and Pd^{II}/UOF-2 (Figure 2h). TEM images showed that the palladium NPs in Pd-reduction were well dispersed and nearly spherical, and their average size was (4.2 ± 0.8) nm, which was slightly smaller than those in Pd⁰/UOF-2 (Figure 8a and b). For comparison, palladium NPs were also directly prepared by reduction of Pd^{II}/UOF-2 with NaBH₄

Table 3. Reduction of various nitroarenes.^[a]

$\text{R-C}_6\text{H}_4\text{-NO}_2 \xrightarrow[\text{H}_2\text{O, 1 h}]{[\text{Pd}], \text{NaBH}_4} \text{R-C}_6\text{H}_4\text{-NH}_2$									
Entry	Reactant	Product	Yield [%] ^[b]	Selectivity [%]	Entry	Reactant	Product	Yield [%] ^[b]	Selectivity [%]
1			100 (98)	100	10			100 (100)	100
2			100 (98)	100	11			100 (96)	100
3			– (96)	96	12			100 (100)	100
4			100 (100)	100	13			100	88
5			100 (92)	100	14			100	84
6			100 (92)	100	15 ^[d]			0	0
7			100 (93)	100	16 ^[e]			0	0
8 ^[c]			– (94)	94	17 ^[f]			100	100
9 ^[c]			– (100)	100					

[a] Unless otherwise stated, the reaction conditions were as follows: substrate (1 mmol), Pd^{II}/UOF-2 (0.5 mol%), and NaBH₄ (3 mmol) in H₂O (2 mL) for 1 h at RT. [b] GC yield, isolated yields are given in parenthesis. [c] THF (0.1 mL) was added. [d] In the absence of Pd^{II}/UOF-2. [e] In the presence of UOF-2 (1.6 mg). [f] In the presence of Pd-NaBH₄ (0.5 mol%).

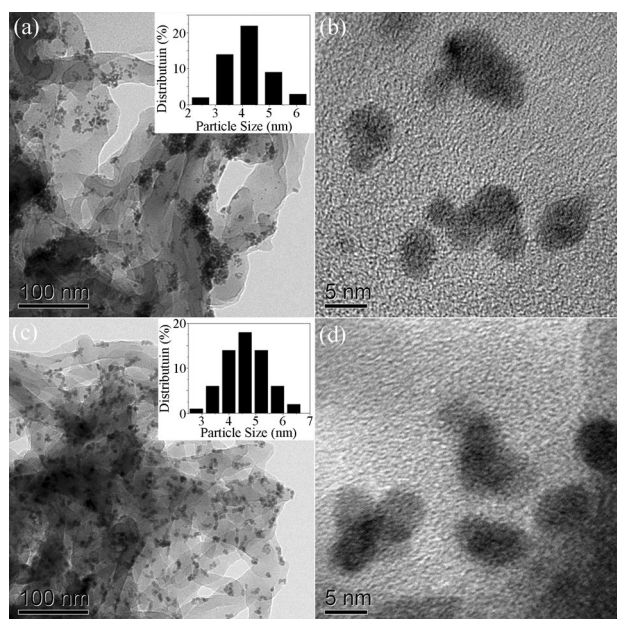


Figure 8. TEM images and Pd size distributions for: a, b) Pd-reduction, and c, d) Pd-NaBH₄.

in H₂O and were denoted as Pd-NaBH₄. TEM analysis showed that Pd-NaBH₄ was nearly spherical with an average size of (4.6 ± 0.6) nm (Figure 8c and d), which was slightly larger than the size of Pd-reduction. The catalytic performance of Pd-NaBH₄ was also investigated in the reduction of nitrobenzene. Nitrobenzene was completely reduced to aniline by NaBH₄ neat water at room temperature in 1 h (Table 3, entry 17).

Conclusion

Two urea-based porous organic frameworks have been successfully prepared by facile urea-forming condensation. They can serve as effective supports for palladium-catalyzed Suzuki–Miyaura cross-coupling reaction and selective reduction of nitroarenes in neat water, excellent catalytic activity and selectivity with negligible palladium leaching were observed. Interestingly, the catalytic reactions can be efficiently performed at room temperature. The superior performances were mainly attributed to good dispersion of urea-based frameworks in water and a microenvironment with high concentration of organic substrates inside the frameworks due to the presence of hydrophilic urea linkage and hydrophobic void. Palladium nanoparticles with narrow size distribution were formed after the catalytic reaction and they are well stabilized by the synergistic effects of the coordination of the urea moiety with palladium and the confinement effect of frameworks. This study not only provides a new approach for the construction of functionalized POFs, but also opens a new avenue to developing heterogeneous catalytic systems in water.

Experimental Section

General information

All chemicals were commercially obtained and used without further purification. ¹H and ¹³C NMR spectra were recorded by using a Bruker AVANCE III NMR spectrometer at 400 and 100 MHz, respectively, with tetramethylsilane (TMS) as an internal standard. Solid-state ¹³C CP/MAS NMR was performed by using a Bruker SB Avance III 500 MHz spectrometer equipped with a 4 mm double-resonance MAS probe, a sample spinning rate of 7.0 kHz, a contact time of 2 ms and pulse delay of 5 s. IR spectra were recorded for KBr pellets by using a Perkin–Elmer Instrument. Thermogravimetric analysis (TGA) was carried out by using a NETZSCH STA 449C instrument and heating samples from 30 to 700 °C in a dynamic nitrogen atmosphere at a heating rate of 10 °C min⁻¹. Powder X-ray diffraction (XRD) patterns were recorded in the range of 2θ = 5–40° by using a desktop X-ray diffractometer (RIGAKU-Miniflex II) with CuK_α radiation (λ = 1.5406 Å). Nitrogen adsorption and desorption isotherms were measured at 77 K by using a Micromeritics ASAP 2020 system. The samples were degassed at 100 °C for 5 h before the measurements. Surface areas were calculated from the adsorption data by using Brunauer–Emmett–Teller (BET) and Langmuir methods. The pore size distribution curves were obtained from the adsorption branches by using a nonlocal density functional theory (NLDFT) method. Field-emission scanning electron microscopy (SEM) was performed by using a JEOL JSM-7500F operated at an accelerating voltage of 3.0 kV. Transmission electron microscope (TEM) images were obtained by using a JEOL JEM-2010 instrument operated at 200 kV. X-ray photoelectron spectroscopy (XPS) measurements were performed by using a Thermo ESCALAB 250 spectrometer with non-monochromatic AlK_α X-rays as the excitation source and with C 1s (284.6 eV) as the reference line. Inductively coupled plasma spectroscopy (ICP) was measured by using a Jobin Yvon Ultima2 instrument. Gas chromatography (GC) was performed by using a Shimadzu GC-2014 equipped with a capillary column (RTX-5, 30 m × 0.25 μm) equipped with a flame ionization detector. Elemental analyses were performed by using an Elementar Vario MICRO Elemental analyzer.

Synthesis of 1,3,5-benzenetriisocyanate

1,3,5-Benzenetriisocyanate was prepared according to a modified literature method.^[28] A solution of 1,3,5-benzenetricarbonyl trichloride (1.0 g, 3.8 mmol) in dry THF (10 mL) was added dropwise to an aqueous solution (10 mL) of sodium azide (1.4 g, 22 mmol) at 0 °C. The reaction mixture was stirred at 0 °C for 2 h to give 1,3,5-benzenetricarbonyl triazide. Toluene (20 mL) and saturated aqueous NaHCO₃ (20 mL) were successively added. After phase separation, the aqueous layer was extracted with toluene (3 × 10 mL). The combined organic layers were successively washed with saturated aqueous solutions of NaHCO₃ and NaCl, and dried over MgSO₄. Subsequently, the toluene layer was gradually heated to 100 °C and stirred till gas evolution stopped. The resultant mixture was concentrated under reduced pressure to give 1,3,5-benzenetriisocyanate as a pale red solid (0.64 g, 85 %). ¹H NMR (400 MHz, CDCl₃): δ = 6.70 ppm (s, 3H); ¹³C NMR (100 MHz, CDCl₃): δ = 135.7, 125.5, 118.6 ppm; FT-IR (KBr): ν̄ = 3091(w), 2261 (vs), 1675 (w), 1614 (s), 1556 (s), 1484 (w), 1320 (w), 1263 (m), 1209 (m), 1100 (m), 898 (m), 853 (m), 665 (m), 562 (m), 452 cm⁻¹ (vw).

Caution! 1,3,5-Benzenetricarbonyl triazide is explosive in the solid state under heating. Therefore, it should preferentially be kept in solution and be handled at 1 g scale maximum.

Synthesis of UOF-1

A solution of 1,4-diaminobenzene (0.45 g, 4.2 mmol) in dry THF (25 mL) was added dropwise to a solution of 1,3,5-benzenetriisocyanate (0.56 g, 2.8 mmol) in toluene (25 mL) at 80 °C. After stirring at 80 °C for 3 d, the precipitate was filtered and successively washed with methanol (2 × 20 mL), THF (2 × 20 mL), and diethyl ether (2 × 20 mL). The residue was dried in vacuo at 80 °C for 12 h to give the target product as a brown powder (0.83 g, 83%). FT-IR (KBr): $\tilde{\nu}$ = 3371 (s), 2257 (w), 1663 (s), 1611 (s), 1545 (s), 1514 (vs), 1445 (m), 1306 (m), 1206 (s), 830 (w), 683 (vw), 512 cm⁻¹ (w); elemental analysis calcd (%) for (C₆H₅N₂O)_n: C 59.50, H 4.16, N 23.13; found: C 56.95, H 5.03, N 21.39.

Synthesis of UOF-2

Following the same procedures as synthesis of UOF-1, UOF-2 was obtained as a brown powder (32% yield). IR (KBr): $\tilde{\nu}$ = 3290 (s), 3105 (w), 2949 (w), 1677 (m), 1609 (s), 1524 (s), 1500 (vs), 1439 (m), 1315 (m), 1280 (m), 1204 (s), 1177 (s), 1004 (vw), 821 (m), 731 (w), 680 (w), 516 cm⁻¹ (w); elemental analysis calcd (%) for (C₉H₇N₂O)_n: C 67.91, H 4.43, N 17.60; found: C 62.30, H 5.13, N 16.89.

Synthesis of Pd^{II}/UOF-1

UOF-1 (0.20 g) was added to a solution of palladium acetate (0.17 g, 0.76 mmol) in dichloromethane (100 mL). The mixture was stirred at RT for 48 h. The resultant solid was isolated by filtration and washed with dichloromethane using a Soxhlet extraction for 24 h, and then dried under vacuum at 80 °C for 12 h to give Pd^{II}/UOF-1 as a gray powder (0.29 g, 80%). The Pd content in Pd^{II}/UOF-1 was 16.87 wt% as determined by ICP. FT-IR (KBr): $\tilde{\nu}$ = 3386 (vs), 1658 (m), 1610 (s), 1560 (s), 1512 (vs), 1427 (s), 1404 (s), 1385 (s), 1332 (m), 1307 (m), 1206 (s), 1050 (w), 1016 (w), 832 (w), 690 (w), 526 cm⁻¹ (w).

Synthesis of Pd^{II}/UOF-2

Following the same procedures as the synthesis of Pd^{II}/UOF-1, Pd^{II}/UOF-2 was obtained as a gray powder (79% yield). The Pd content in Pd^{II}/UOF-2 was 16.83 wt% as determined by ICP. FT-IR (KBr): $\tilde{\nu}$ = 3396 (vs), 1650 (s), 1610 (s), 1499 (vs), 1429 (s), 1384 (s), 1320 (s), 1205 (s), 1178 (s), 1049 (w), 821 (w), 713 (w), 689 (w), 552 (vw), 526 cm⁻¹ (vw).

General procedures for the Suzuki–Miyaura cross-coupling reaction

Pd^{II}/UOF-1 or Pd^{II}/UOF-2 (0.5 mol%) was added to a mixture of aryl bromide (0.5 mmol), arylboronic acid (0.75 mmol), and base (1.0 mmol) in water (2.0 mL). After the mixture was stirred in a pre-heated oil bath (60 °C) for the appropriate time, the resultant mixture was cooled in ice water and the product was extracted with ethyl acetate (3 × 5 mL). The combined organic layer was dried and concentrated under reduced pressure. The crude products were further purified by flash column chromatography on silica gel to afford the desired products. The identity of the products was confirmed by comparison with literature spectroscopic data.

Reuse of Pd^{II}/UOF-1 and Pd^{II}/UOF-2 in the Suzuki–Miyaura cross-coupling reaction

After the Suzuki–Miyaura cross-coupling reaction was performed in the presence of Pd^{II}/UOF-1 or Pd^{II}/UOF-2 (0.5 mol%), 4-bromophe-

nol (87 mg, 0.5 mmol), phenylboronic acid (92 mg, 0.75 mmol), and K₂CO₃ (138 mg, 1.0 mmol) in water (2.0 mL) at 60 °C for 3 h, the mixture was cooled in ice water and was extracted with ethyl acetate (3 × 5 mL). The combined organic layer was analyzed by using GC. The gray powder in the aqueous phase was separated by centrifugation, washed thoroughly with water, and then used for the next run.

General procedures for reduction of nitroarenes

NaBH₄ (114 mg, 3 mmol) was added in one portion to a stirred aqueous solution (2 mL) of nitroarenes (1.0 mmol) and Pd^{II}/UOF-1 or Pd^{II}/UOF-2 (0.5 mol%) at RT. After 1 h, the resultant mixture was extracted with diethyl ether (3 × 5 mL). The combined organic layer was analyzed by using GC, and concentrated under reduced pressure to give the target products. The identity of the products was confirmed by comparison with GC retention time of commercial materials and literature NMR spectroscopic data.

Reuse of Pd^{II}/UOF-1 and Pd^{II}/UOF-2 in the reduction of nitroarenes

After the reduction of nitrobenzene was complete, the resultant mixture was extracted with diethyl ether (3 × 5 mL). The combined organic layer was determined by using GC analysis. The gray powder in the aqueous phase was separated by centrifugation, washed with water thoroughly, and then used for the next run.

Synthesis of Pd⁰/UOF-1 and Pd⁰/UOF-2

After the cross-coupling reaction between 4-bromoacetophenone and phenylboronic acid in the presence of Pd^{II}/UOF-1 or Pd^{II}/UOF-2 was complete, the resultant mixture was extracted with diethyl ether (3 × 5 mL). The residual suspension was centrifuged and washed thoroughly with ethanol to afford Pd⁰/UOF-1 or Pd⁰/UOF-2 as gray powders.

Synthesis of Pd-reduction

After the reduction of nitrobenzene was finished, the resultant mixture was extracted with diethyl ether (3 × 5 mL). The residues were centrifuged, washed thoroughly with water and ethanol to afford Pd-reduction as a gray powder.

Synthesis of Pd-NaBH₄

An aqueous solution of NaBH₄ (0.1 M, 114 mg, 3.0 mmol) was rapidly added to a stirred suspension of Pd^{II}/UOF-2 (3.1 mg) in water (2 mL). After 5 min, the resultant suspension was centrifuged and washed thoroughly with ethanol to afford Pd-NaBH₄ as a gray powder.

Acknowledgements

The authors acknowledge the 973 Program (2011CBA00502, 2010CB933501), the National Natural Science Foundation of China (21273239) and the "One Hundred Talent Project" from the Chinese Academy of Sciences for financial support.

Keywords: heterogeneous catalysis · palladium · porous organic frameworks · urea · water chemistry

- [1] a) Z. H. Xiang, D. P. Cao, *J. Mater. Chem. A* **2013**, *1*, 2691–2718; b) Y. H. Jin, Y. L. Zhu, W. Zhang, *CrystEngComm* **2013**, *15*, 1484–1499; c) R. Dawson, A. I. Cooper, D. J. Adams, *Prog. Polym. Sci.* **2012**, *37*, 530–563.
- [2] a) P. Pachfule, V. M. Dhavale, S. Kandambeth, S. Kurungot, R. Banerjee, *Chem. Eur. J.* **2013**, *19*, 974–980; b) H. Yu, C. Shen, M. Tian, J. Qu, Z. Wang, *Macromolecules* **2012**, *45*, 5140–5150; c) Z. Chang, D. S. Zhang, Q. Chen, X. H. Bu, *Phys. Chem. Chem. Phys.* **2013**, *15*, 5430–5442; d) S. Y. Ding, W. Wang, *Chem. Soc. Rev.* **2013**, *42*, 548–568; e) Y. Yuan, H. Ren, F. Sun, X. Jing, K. Cai, X. Zhao, Y. Wang, Y. Wei, G. Zhu, *J. Phys. Chem. C* **2012**, *116*, 26431–26435; f) H. Ren, T. Ben, F. Sun, M. Guo, X. Jing, H. Ma, K. Cai, S. Qiu, G. Zhu, *J. Mater. Chem.* **2011**, *21*, 10348; g) M. H. Weston, G. W. Peterson, M. A. Browe, P. Jones, O. K. Farha, J. T. Hupp, S. T. Nguyen, *Chem. Commun.* **2013**, *49*, 2995–2997.
- [3] a) S. Ren, M. J. Bojdy, R. Dawson, A. Laybourn, Y. Z. Khimyak, D. J. Adams, A. I. Cooper, *Adv. Mater.* **2012**, *24*, 2357–2361; b) S. Xu, Y. Luo, B. Tan, *Macromol. Rapid Commun.* **2013**, *34*, 471–484; c) T. Ben, S. Qiu, *CrystEngComm* **2013**, *15*, 17–26; d) D. Yuan, W. Lu, D. Zhao, H. C. Zhou, *Adv. Mater.* **2011**, *23*, 3723–3725; e) X. Q. Zou, H. Ren, G. S. Zhu, *Chem. Commun.* **2013**, *49*, 3925–3936; f) W. Lu, J. P. Sculley, D. Yuan, R. Krishna, Z. Wei, H. C. Zhou, *Angew. Chem.* **2012**, *124*, 7598–7602; *Angew. Chem. Int. Ed.* **2012**, *51*, 7480–7484; g) H. Zhao, Z. Jin, H. Su, J. Zhang, X. Yao, H. Zhao, G. Zhu, *Chem. Commun.* **2013**, *49*, 2780–2782; h) X. Zhu, C. Tian, S. M. Mahurin, S. H. Chai, C. Wang, S. Brown, G. M. Veith, H. Luo, H. Liu, S. Dai, *J. Am. Chem. Soc.* **2012**, *134*, 10478–10484; i) W. G. Lu, D. Q. Yuan, J. L. Sculley, D. Zhao, R. Krishna, H. C. Zhou, *J. Am. Chem. Soc.* **2011**, *133*, 18126–18129.
- [4] a) J. X. Jiang, C. Wang, A. Laybourn, T. Hasell, R. Clowes, Y. Z. Khimyak, J. Xiao, S. J. Higgins, D. J. Adams, A. I. Cooper, *Angew. Chem.* **2011**, *123*, 1104–1107; *Angew. Chem. Int. Ed.* **2011**, *50*, 1072–1075; b) Z. Xie, C. Wang, K. E. deKrafft, W. Lin, *J. Am. Chem. Soc.* **2011**, *133*, 2056–2059.
- [5] a) R. Palkovits, M. Antonietti, P. Kuhn, A. Thomas, F. Schuth, *Angew. Chem.* **2009**, *121*, 7042–7045; *Angew. Chem. Int. Ed.* **2009**, *48*, 6909–6912; b) C. E. Chan-Thaw, A. Villa, P. Katekomol, D. Su, A. Thomas, L. Prati, *Nano Lett.* **2010**, *10*, 537–541; c) C. E. Chan-Thaw, A. Villa, L. Prati, A. Thomas, *Chem. Eur. J.* **2011**, *17*, 1052–1057.
- [6] a) L. Chen, Y. Yang, D. Jiang, *J. Am. Chem. Soc.* **2010**, *132*, 9138–9143; b) A. M. Shultz, O. K. Farha, J. T. Hupp, S. T. Nguyen, *Chem. Sci.* **2011**, *2*, 686.
- [7] a) S. Y. Ding, J. Gao, Q. Wang, Y. Zhang, W. G. Song, C. Y. Su, W. Wang, *J. Am. Chem. Soc.* **2011**, *133*, 19816–19822; b) M. K. Bhunia, S. K. Das, P. Pachfule, R. Banerjee, A. Bhaumik, *Dalton Trans.* **2012**, *41*, 1304–1311.
- [8] a) Y. Xie, T. T. Wang, X. H. Liu, K. Zou, W. Q. Deng, *Nat. Commun.* **2013**, *4*, 1960–1967; b) J. Chun, S. Kang, N. Kang, S. M. Lee, H. J. Kim, S. U. Son, *J. Mater. Chem. A* **2013**, *1*, 5517–5523.
- [9] a) P. Kaur, J. T. Hupp, S. T. Nguyen, *ACS Catal.* **2011**, *1*, 819–835; b) Y. G. Zhang, S. N. Riduan, *Chem. Soc. Rev.* **2012**, *41*, 2083–2094.
- [10] R. N. Butler, A. G. Coyne, *Chem. Rev.* **2010**, *110*, 6302–6337.
- [11] R. Dawson, A. Laybourn, R. Clowes, Y. Z. Khimyak, D. J. Adams, A. I. Cooper, *Macromolecules* **2009**, *42*, 8809–8816.
- [12] a) M. Rose, N. Klein, W. Bohlmann, B. Bohringer, S. Fichtner, S. Kaskel, *Soft Matter* **2010**, *6*, 3918–3923; b) M. R. Liebl, J. Senker, *Chem. Mater.* **2013**, *25*, 970–980; c) Z. J. Yan, H. Ren, H. P. Ma, R. R. Yuan, Y. Yuan, X. Q. Zou, F. X. Sun, G. S. Zhu, *Microporous Mesoporous Mater.* **2013**, *173*, 92–98.
- [13] S. Y. Moon, J. S. Bae, E. Jeon, J. W. Park, *Angew. Chem.* **2010**, *122*, 9694–9698; *Angew. Chem. Int. Ed.* **2010**, *49*, 9504–9508.
- [14] a) S. S. Lee, S. N. Riduan, N. Erathodiyil, J. Lim, J. L. Cheong, J. H. Cha, Y. Han, J. Y. Ying, *Chem. Eur. J.* **2012**, *18*, 7394–7403; b) J. Y. Shin, B. S. Lee, Y. Jung, S. J. Kim, S. G. Lee, *Chem. Commun.* **2007**, 5238–5240.
- [15] T. Harada, S. Ikeda, Y. H. Ng, T. Sakata, H. Mori, T. Torimoto, M. Matsu-mura, *Adv. Funct. Mater.* **2008**, *18*, 2190–2196.
- [16] a) F. Z. Kong, C. S. Zhou, J. Y. Wang, Z. Y. Yu, R. H. Wang, *ChemPlusChem* **2013**, *78*, 536–545; b) L. Y. Li, J. Y. Wang, C. S. Zhou, R. H. Wang, M. C. Hong, *Green Chem.* **2011**, *13*, 2071–2077; c) C. S. Zhou, J. Y. Wang, L. Y. Li, R. H. Wang, M. C. Hong, *Green Chem.* **2011**, *13*, 2100–2106; d) D. Zhang, C. S. Zhou, R. H. Wang, *Catal. Commun.* **2012**, *22*, 83–88.
- [17] L. Y. Li, J. Y. Wang, T. Wu, R. H. Wang, *Chem. Eur. J.* **2012**, *18*, 7842–7851.
- [18] a) J. X. Jiang, F. Su, H. Niu, C. D. Wood, N. L. Campbell, Y. Z. Khimyak, A. I. Cooper, *Chem. Commun.* **2008**, 486–488; b) T. Ben, C. Pei, D. Zhang, J. Xu, F. Deng, X. Jing, S. Qiu, *Energy Environ. Sci.* **2011**, *4*, 3991–3999; c) A. P. Katsoulidis, M. G. Kanatzidis, *Chem. Mater.* **2011**, *23*, 1818–1824; d) L. Chen, Y. Honsho, S. Seki, D. Jiang, *J. Am. Chem. Soc.* **2010**, *132*, 6742–6748.
- [19] K. S. W. Sing, D. H. Everett, R. A. W. Haul, L. Moscou, R. A. Pierotti, J. Rouquerol, T. Siemieniowska, *Pure Appl. Chem.* **1985**, *57*, 603–619.
- [20] J. Weber, J. Schmidt, A. Thomas, W. Bohlmann, *Langmuir* **2010**, *26*, 15650–15656.
- [21] A. P. Katsoulidis, M. G. Kanatzidis, *Chem. Mater.* **2012**, *24*, 471–479.
- [22] P. J. Ellis, I. J. Fairlamb, S. F. Hackett, K. Wilson, A. F. Lee, *Angew. Chem.* **2010**, *122*, 1864–1868; *Angew. Chem. Int. Ed.* **2010**, *49*, 1820–1824.
- [23] B. Inés, R. SanMartin, M. J. Moure, E. Domínguez, *Adv. Synth. Catal.* **2009**, *351*, 2124–2132.
- [24] M. Lamblin, L. Nassar-Hardy, J.-C. Hierso, E. Fouquet, F.-X. Felpin, *Adv. Synth. Catal.* **2010**, *352*, 33–79.
- [25] N. T. S. Phan, M. Van Der Sluys, C. W. Jones, *Adv. Synth. Catal.* **2006**, *348*, 609–679.
- [26] a) A. El Kadib, K. McEleney, T. Seki, T. K. Wood, C. M. Crudden, *Chem-CatChem* **2011**, *3*, 1281–1285; b) I. Thomé, A. Nijs, C. Bolm, *Chem. Soc. Rev.* **2012**, *41*, 979–987.
- [27] a) M. O'Connor, A. Kellett, M. McCann, G. Rosair, M. McNamara, O. Howe, B. S. Creaven, S. McClean, A. F. A. Kia, D. O'Shea, M. Devereux, *J. Med. Chem.* **2012**, *55*, 1957–1968; b) K. Bao, Y. Dai, Z. B. Zhu, F. J. Tu, W. G. Zhang, X. S. Yao, *Bioorg. Med. Chem.* **2010**, *18*, 6708–6714; c) S. L. Adamski-Werner, S. K. Palaninathan, J. C. Sacchettini, J. W. Kelly, *J. Med. Chem.* **2004**, *47*, 355–374.
- [28] M. de Loos, J. H. van Esch, R. M. Kellogg, B. L. Feringa, *Tetrahedron* **2007**, *63*, 7285–7301.

Received: October 16, 2013

Revised: December 16, 2013

Published online on February 20, 2014